

Experimental report

09/02/2016

Proposal: 4-01-1431

Council: 10/2014

Title: Longitudinal spin fluctuation in Ca₂RuO₄

Research area: Physics

This proposal is a new proposal

Main proposer: Anil JAIN

Experimental team: Maximilian Josef KRAUTLOHER
Dmytro INOSOV
Juan Pablo PORRAS PEREZ GUERRERO
Bumjoon KIM
Anil JAIN

Local contacts: Alexandre IVANOV

Samples: Ca₂RuO₄

Instrument	Requested days	Allocated days	From	To
IN20	8	8	21/07/2015	29/07/2015

Abstract:

The phenomenon of Bose-Einstein condensation (BEC) takes many different guises in nature ranging from superfluidity in liquid helium and ultracold atomic gases to superconductivity in metals. An analogy is also found in magnetic insulators, in which a quantum phase transition takes place as magnons condensate. A well-known example is the BEC of triplons in a dimer system TiCuCl₃ induced by tuning the boson density using magnetic field, providing a connection between complex quantum properties of matter and BEC. Recently, a novel type of BEC of spin-orbit excitons has been proposed in Ca₂RuO₄. Using the unpolarized neutron scattering measurements, we have observed a dispersive magnon branch (up to 41 meV) with a gap of 12 meV along the [H00]-direction in Ca₂RuO₄. In addition, an almost non-dispersive magnon branch has also been observed at ~42 meV, which appears to be arising from the longitudinal magnetic fluctuations. Aim of the proposed experiment is to separate the spectra of transverse and longitudinal magnetic fluctuations by the polarized inelastic neutron scattering measurements.

Higgs amplitude mode and its decay in a two dimensional antiferromagnet

A. Jain^{1,2,†}, M. Krautloher^{1,†}, J. Porras^{1,†}, G. H. Ryu¹, D. P. Chen¹, D. L. Abernathy³,
J. T. Park⁴, A. Ivanov⁵, J. Chaloupka⁶, G. Khaliullin¹, B. Keimer¹, and B. J. Kim^{1,*}

¹Max Planck Institute for Solid State Research, Heisenbergstraße 1, D-70569 Stuttgart, Germany

²Solid State Physics Division, Bhabha Atomic Research Centre, Mumbai 400085, India

³Quantum Condensed Matter Division, Oak Ridge National Laboratory, Oak Ridge, Tennessee 37831, USA

⁴Heinz Maier-Leibnitz Zentrum, TU München, Lichtenbergstraße 1, D-85747 Garching, Germany

⁵Institut Laue-Langevin, 6, rue Jules Horowitz, BP 156, 38042 Grenoble Cedex 9, France and

⁶Central European Institute of Technology, Masaryk University, Kotlářská 2, 61137 Brno, Czech Republic

(Dated: February 9, 2016)

Condensed-matter analogs of the Higgs boson in particle physics allow access to its behavior in varying symmetry and dimensionality[?]. Evidence for the Higgs mode has been reported in a number of different settings, including the ultracold atomic gas[?], disordered superconductor[?], and dimerized quantum magnet[?]. However, the dynamics of the Higgs mode in low dimension remains unclear due to the lack of a suitable material system coupled to a direct experimental probe. Here, we discover and study the Higgs mode in a two-dimensional antiferromagnet using spin-polarized inelastic neutron scattering. Our spin-wave spectra of Ca_2RuO_4 directly reveal a well-defined longitudinal Higgs mode, which, however, at the wavevector of the minimum energy gap quickly decays into transverse Goldstone modes. Through a complete mapping of the transverse modes in the reciprocal space, we uniquely specify the minimal model Hamiltonian and describe the decay process. Our result establishes the first condensed matter system to study the detailed dynamics of the Higgs mode in two dimension.

For a system of interacting spins, the amplitude fluctuation of the local magnetization—the Higgs mode—can exist as a well-defined collective excitation near a quantum critical point (QCP). We consider here the magnetic instability driven by intra-ionic spin-orbit coupling, which tends toward a nonmagnetic state through complete cancellation of orbital (L) and spin (S) moments when they are of equal magnitude[?][?]. Specifically, we investigate the magnetic insulator Ca_2RuO_4 , a quasi-two-dimensional antiferromagnet[?] with nominally $L=1$ and $S=1$ (Fig. 1). Because the local symmetry around the Ru(IV) ion is very low[?][?] (having only inversion symmetry), it is widely believed that the orbital moment is completely quenched by the crystalline electric field[?][?][?], which is mostly contributed by the compressive distortion of the RuO_6 octahedra along the c -axis, parametrized by Δ . In the absence of orbital moment, the nearest-neighbor magnetic exchange interaction is necessarily isotropic, which would be manifest as the Heisenberg dispersion relation of the spin wave. Any deviation from it implies an unquenched orbital moment,

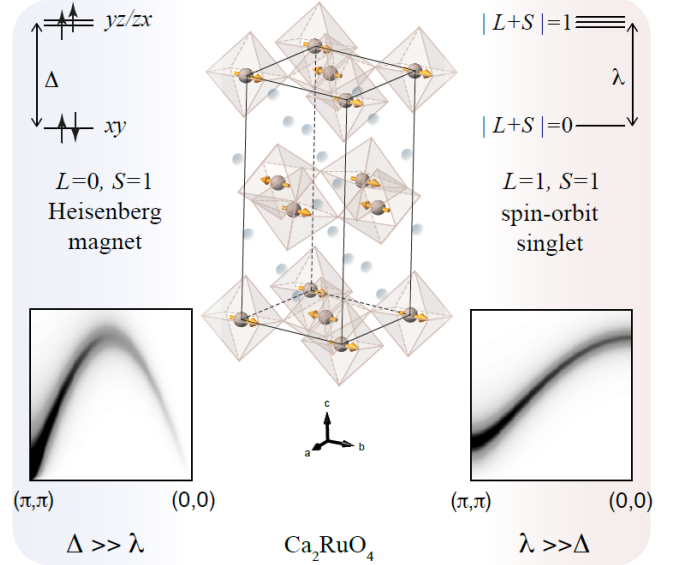


FIG. 1. **Crystal, magnetic, and electronic structures of Ca_2RuO_4 .** Ca_2RuO_4 crystallizes in the orthorhombic Pbca space group, a distorted variant of the layered perovskite structure with a quasi-two-dimensional square lattice. The distortion involves 2% compression of the RuO_6 octahedra along the c -axis, and their rotation and tilting about the same axis. (π, π) magnetic order develops below $T_N \approx 110$ K with the moment (orange arrow) aligned approximately along the b -axis. The compressive distortion of the RuO_6 leads to the splitting Δ between the orbitals of xy and yz/zx symmetry. If Δ is much larger than the spin-orbit coupling (λ), the orbital degrees of freedom is completely quenched and $S=1$ Heisenberg magnet is obtained. In the other limit $\Delta \ll \lambda$, a singlet ground state is stabilized, which is non-magnetic. These two distinct magnetic phases have excitation spectra qualitatively different from each other. See Fig. S1 and Fig. S2 for the evolution of the electronic structure and the spin-wave dispersions in between these two limiting cases.

the magnitude of which will determine the extent of the relevance of Ca_2RuO_4 to the Higgs physics.

Our comprehensive set of time-of-flight (TOF) inelastic neutron scattering (INS) data over the full Brillouin zone (Fig. 2a) shows that the transverse spin-wave dispersion qualitatively deviates from that of a Heisenberg antiferromagnet. In particular, the dispersion has the global

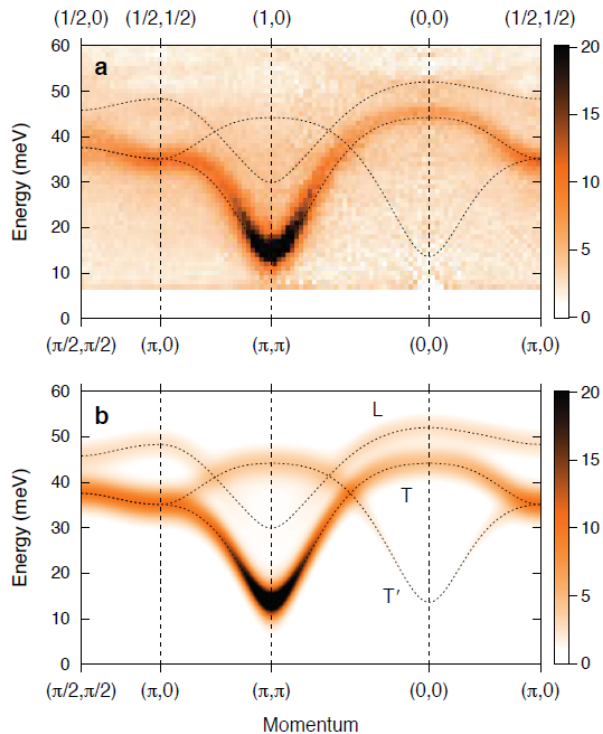


FIG. 2. **Spin-wave dispersion strongly deviating from the Heisenberg model.** **a**, TOF INS spectra along high symmetry directions (see Fig. S3 for more details). The dotted lines are from panel **b** for direct comparison between theory and experiment. **b**, The excitation spectra of the model in eq. (1) calculated with the parameters $E \simeq 25$ meV, $J \simeq 5.8$ meV, $\epsilon \simeq 4.0$ meV, $\alpha = 0.15$, and $A \simeq 2.3$ meV. The spectra were convoluted with Gaussian function of 2.5 meV full-width half-maximum to account for the instrument energy resolution. Transverse and longitudinal modes are labeled as “T” and “L”, respectively. T’ mode arises from back-folding of the T mode by the magnetic (π, π) scattering. The intensities in panel **a** and **b** are in the same arbitrary units.

maximum at $\mathbf{q} = (0,0)$, in sharp contrast to a Heisenberg antiferromagnet having a minimum there (Fig. 1). This is a clear manifestation of orbital magnetism^{???}, which leads us to consider the other limit of strong spin-orbit coupling described in terms of a singlet and a triplet separated in energy by λ (Fig. 1). In this limit, the ground state is nonmagnetic with zero total angular momentum, and therefore a QCP separating it from a magnetically ordered phase is in principle expected. In reality, this QCP can be pre-empted by a Mott transition or rendered a first-order transition by, e.g., coupling to the lattice, but for our purpose it is sufficient if the system is reasonably close to the hypothetical QCP.

To assess the proximity to the QCP and the possibility of finding the Higgs mode, we first reproduce the observed transverse spin-wave mode by applying the linear spin-wave theory^{???} to the following phenomenological Hamiltonian obtained from symmetry considerations,

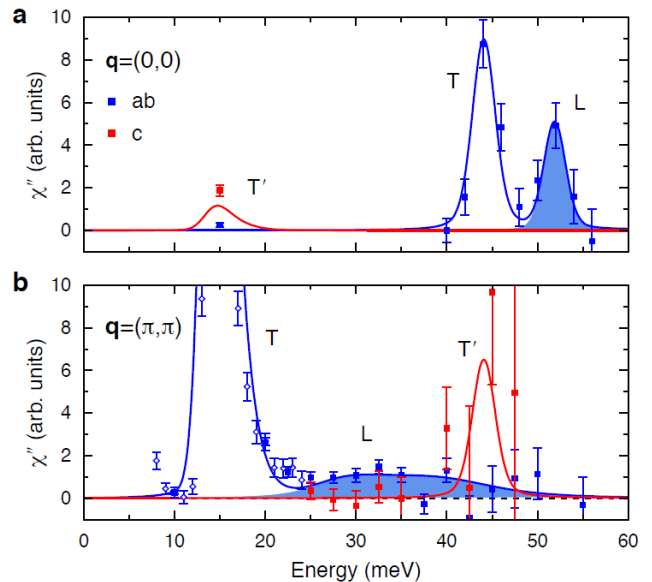


FIG. 3. **Identification of the magnetic modes with polarized INS and their comparison to model calculation.** Imaginary part of the dynamic spin susceptibility obtained by normalising the INS spectra measured at **a**, $\mathbf{q} = (0,0)$ (Fig. S5) and **b**, $\mathbf{q} = (\pi, \pi)$ (Fig. S6) with respect to the orientation factor and the isotropic form factor for Ru^+ (Fig. S4). Blue (red) symbols indicate in-plane (out-of-plane) polarized magnetic intensities. Solid symbols show data with the background removed by taking the difference between two spin-flip channels, and open symbols show data from a single spin-flip channel.

written as:

$$\begin{aligned}
 H = & J \sum_{\langle ij \rangle} (\mathbf{S}_i \cdot \mathbf{S}_j - \alpha S_{zi} S_{zj}) + E \sum_i S_{zi}^2 + \epsilon \sum_i S_{xi}^2 \\
 & \mp A \sum_{\langle ij \rangle} (S_{xi} S_{yj} + S_{yi} S_{xj}). \quad (1)
 \end{aligned}$$

Here, \mathbf{S} denotes the pseudospin with entangled spin and orbital degrees of freedom as required by the sizable spin-orbit coupling manifest as the anomalous spin-wave dispersion. This model includes single-ion anisotropy (E and ϵ) terms induced by tetragonal ($z \parallel c$) and orthorhombic ($x \parallel a$) distortions, correspondingly, as well as the XY-type exchange anisotropy ($\alpha > 0$) and the bond-directional pseudodipolar interaction (A); note that its sign depends on the bond. Also symmetry allowed but neglected are the Dzyaloshinskii-Moriya interaction (which can be gauged out by a suitable local coordinate transformation) and further-neighbor interactions. These coupling constants are determined by fitting the model to the measure spectra (provided in the caption of Fig. 2). We stress that this model gives the unique minimal description of the system, which we also derive explicitly starting from the microscopic electronic structure.

Our calculation (Fig. 2b) predicts in this parameter

regime an intense Higgs amplitude mode, which heralds a proximate quantum critical point.

Armed with the specific guidance, we pursue the Higgs mode using spin-polarized INS, using the scattering geometry that maximizes the neutron cross section for the Higgs mode. We use the standard XYZ-difference method to filter out all non-magnetic and incoherent scattering signals and to resolve three polarizations of the spin wave: the Higgs amplitude mode, or the longitudinal mode (L) oscillates along b crystallographic axis, and the transverse Goldstone modes (T and T') along a and c axes. Because our sample mosaic consisting of ~ 100 crystals is "twinned", i.e., approximately half of them are rotated 90° about the c axis with respect to the other half, we can only distinguish between the in-plane (ab) polarized mode and out-of-plane (c) polarized mode. However, this is sufficient to identify the Higgs mode.

Figure 3a shows the measured (symbols with error bars) and calculated (solid lines) dynamical susceptibility at $\mathbf{q} = (0,0)$. We observe three peaks in total as expected, but not all of them were clearly seen in the TOF data because of different optimal scattering geometries they appear in. The highest-energy peak at ≈ 52 meV is unambiguously identified as the Higgs mode by its magnetic and in-plane-polarized nature, because the second in-plane-polarized mode of lower energy at ≈ 45 meV has already been identified as the T mode (Fig. 2). Further, the data is in excellent accord with the model calculation, which has no adjustable parameter after fitting to the dispersion of the T mode. The intensity ratio between the L and T modes is about 0.55 ± 0.11 , which is a quantitative measure of the proximity to the QCP (Fig. S7), at which the distinction between the L and T modes vanishes and their intensity becomes identical.

Having established the existence of the Higgs amplitude mode, we now look at its long-wavelength behavior. It is at the ordering wave vector where the stability of the Higgs mode critically depends on the dimensionality of the system. In three dimension, earlier INS studies on a dimerized quantum magnet have established a well-defined Higgs mode⁷, which was then used to study its critical behavior across a QCP⁷. In sharp contrast, our in-plane polarized spectrum measured at $\mathbf{q} = (\pi, \pi)$ shows only one clear peak for the T mode at ≈ 14 meV, followed by a broad distribution in the energy range 20-50 meV of magnetic intensities, which are well outside of the error bar from zero intensity. The Higgs mode has decayed to the extent that its trace is barely visible even in the spin-polarized INS spectrum.

However, it is also known that the response of the Higgs mode strongly depends on the symmetry of the probe being used. Therefore, its rapid decay in the longitudinal susceptibility measured by INS is not to be taken as conclusive of its instability in two dimension. In fact, it has been shown in other two-dimensional systems, such as the disordered superconductor⁷ and superfluid of cold atom gas⁷, that the Higgs mode is clearly visible in the

scalar susceptibility with its characteristic $\sim \omega^3$ dependence of its onset in the energy spectrum. Indeed, theory predicts that the Higgs mode in the longitudinal susceptibility quickly loses its coherence by decaying into a pair of Goldstone modes⁷, which results in an infrared divergence in two dimension and renders the Higgs mode elusive.

Conversely, the INS spectrum $\mathbf{q} = (\pi, \pi)$ encodes detailed information on the decay process of the Higgs mode that are not available from other measurements. To model the decay process, we go beyond the harmonic approximation to include the coupling of the longitudinal mode to the two-magnon continuum. The solid lines in Fig. 3 shows the result of the final calculation, which gives an excellent description of the data both at $\mathbf{q} = (0,0)$ and $\mathbf{q} = (\pi, \pi)$; the decay process is kinematically restricted away from the ordering wave vector, and the Higgs mode is well identified at $\mathbf{q} = (0,0)$.

Intriguingly, we encounter a rather unusual situation where even all the transverse modes are massive (gapped), as a result of orthorhombic symmetry of the crystal structure parameterized by ϵ . This finite transverse gap cuts off the infrared singularity and the spectral weight piles up at a finite energy. We illustrate this point in Fig. 4 by simulating the change in the longitudinal spectrum as the system approaches the QCP. At $\mathbf{q} = (\pi, \pi)$, the decay of the Higgs mode into a pair of minimum-energy transverse modes is still the dominant channel, which generates a 'resonance' at the twice the energy of the gap. This resonance steals much of the spectral weight from the longitudinal mode obscuring its feature especially near the QCP. When ϵ is set to zero, we recover the infrared divergence (dotted lines). As the system moves away from the QCP, the longitudinal mode progressively hardens and becomes weaker, and its spectral weight spans a larger energy range. The spectral evolution at $\mathbf{q} = (0,0)$ shows this trend with the decay process suppressed; the Higgs mode remains a well-defined excitation far way from the QCP although its intensity quickly diminishes.

At this point, it is uncertain if the decay process considered above fully describes the dynamics. It is conceivable that the Higgs mode can also decay into other vortex-like excitations in two dimension. Now that we have established a two-dimensional material system, future studies can further reveal its details. In particular, it would be interesting to compare the results presented herein with the spectra from resonant inelastic x-ray scattering, which can in principle access both the scalar and longitudinal susceptibility. Finally, it is interesting to note that the Higgs boson in particle physics is detected through its decay products, such as a pair of photons, W bosons, Z bosons, or leptons; and, in fact, the Higgs boson is established through the decay rates and branching ratio of these processes, which have been calculated to very high precision. Our study represents the first step toward a parallel development in condensed matter physics.